



OPEN

Diffusion Tensor Imaging Reveals Acute Subcortical Changes after Mild Blast-Induced Traumatic Brain Injury

SUBJECT AREAS:
WHITE MATTER INJURY
NEURODEGENERATION

Received
29 January 2014

Accepted
27 March 2014

Published
2 May 2014

Correspondence and
requests for materials
should be addressed to
D.V.A. (denes.
agoston@usuhs.edu.)

* Current address:
Department of
Neurosurgery, VA
Medical Center-
Research 151,
Medical College of
Wisconsin, 5000
West National Ave.,
Milwaukee, WI
53295.

Alaa Kamnakhsh^{1,2}, Matthew D. Budde^{3*}, Erzsebet Kovcsdi⁴, Joseph B. Long⁵, Joseph A. Frank³
& Denes V. Agoston¹

¹Department of Anatomy, Physiology and Genetics, The Uniformed Services University, 4301 Jones Bridge Road, Bethesda, MD 20814, ²Center for Neuroscience and Regenerative Medicine, The Uniformed Services University, 4301 Jones Bridge Road, Bethesda, MD 20814, ³Radiology and Imaging Sciences, National Institute of Biomedical Imaging and Bioengineering, National Institutes of Health, Room B1N256 MSC 1074, 10 Center Drive, Bethesda, MD 20892, ⁴US Department of Veterans Affairs, Veterans Affairs Central Office, 810 Vermont Avenue NW, Washington, DC 20420, ⁵Blast-Induced Neurotrauma Branch, Center for Military Psychiatry and Neuroscience, Walter Reed Army Institute of Research, 503 Robert Grant Avenue, Silver Spring, MD 20910.

Mild blast-induced traumatic brain injury (mbTBI) poses special diagnostic challenges due to its overlapping symptomatology with other neuropsychiatric conditions and the lack of objective outcome measures. Diffusion tensor imaging (DTI) can potentially provide clinically relevant information toward a differential diagnosis. In this study, we aimed to determine if single and repeated (5 total; administered on consecutive days) mild blast overpressure exposure results in detectable structural changes in the brain, especially in the hippocampus. Fixed rat brains were analyzed by ex vivo DTI at 2 h and 42 days after blast (or sham) exposure(s). An anatomy-based region of interest analysis revealed significant interactions in axial and radial diffusivity in a number of subcortical structures at 2 h only. Differences between single- and multiple-injured rats were largely in the thalamus but not the hippocampus. Our findings demonstrate the value and the limitations of DTI in providing a better understanding of mbTBI pathobiology.

Mild traumatic brain injury (mTBI) continues to be the least understood form of traumatic brain injury (TBI) despite its high incidence and substantial toll on patients and health care systems¹. In the military, mTBIs are mostly caused by the exposure to low levels of blast from improvised explosive devices resulting in mild blast-induced TBI (mbTBI)²⁻⁴. The diagnosis of mbTBI currently relies on subjective assessments and self-reports of symptoms such as disorientation, altered states of consciousness, headaches, and emotional and cognitive dysfunction—all of which are involved in post-traumatic stress disorder (PTSD)⁵. Because of the mild and transient nature of symptoms that follow mbTBI, soldiers typically return to duty and are frequently re-exposed to additional mild blasts. Studies have suggested that repeated mbTBI is a risk factor for developing late onset neurodegenerative conditions such as chronic traumatic encephalopathy (CTE)⁶.

Objective outcome measures can provide especially valuable, clinically relevant information in a non-/minimally invasive and repeatable manner. Various modalities of magnetic resonance imaging (MRI), including diffusion tensor imaging (DTI), have been utilized in clinical settings following TBI⁷⁻¹⁰. However, only a limited number of clinical studies included readouts at several post-injury time points in Veterans¹¹⁻¹⁷. DTI's sensitivity relative to conventional imaging tools has prompted its recent use in experimental mTBI¹⁸⁻²⁰ with a few rodent blast-induced TBI (bTBI) studies²¹⁻²⁴. These studies identified a number of brain regions, including the hippocampus and the cerebellum, as being affected in mbTBI²⁵. Injury-induced changes in serum, cerebrospinal fluid, and tissue protein biomarker levels have also been extensively investigated in both clinical and experimental TBI²⁶⁻²⁸. Together, imaging and molecular biomarkers would enable the monitoring of pathological processes over time and allow for more direct comparisons between experimental findings and clinical TBI cases.

The full potential and limitations of using imaging and molecular biomarkers in the diagnosis and monitoring of TBIs, especially mTBIs, are currently unknown due to a substantial gap between clinical and experimental findings and their translatability²⁹. Furthermore, our understanding of how structural changes relate to cellular, molecular, and functional changes in TBI is very limited. Our previous works using the rodent model of single and repeated mbTBI recapitulated some of the behavioral changes that are observed in human bTBI³⁰. Using histo-

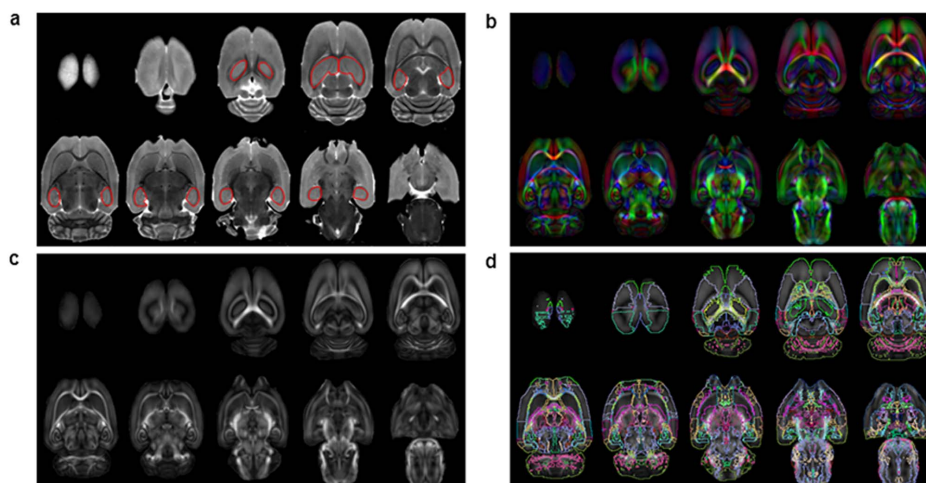


Figure 1 | MRI data analysis. (a) A T2-weighted image from a single subject with the hippocampus manually outlined in red. (b) A mean directionally encoded color image. (c) Map of FA derived from DTI of all spatially registered brains (every second slice is shown). (d) The registered anatomical ROIs derived from the atlas overlaid on the FA map for visualization.

logic and proteomic analyses of functionally relevant brain regions and peripheral blood, we identified several pathologies at different post-injury time points. These include neuronal and glial damage and/or death, axonal damage, metabolic and vascular changes, and inflammation. Additionally, we identified several pathologies that include neuronal and glial damage and/or death, axonal damage, metabolic and vascular changes, and inflammation at different post-injury time points using histologic and proteomic analyses of functionally relevant brain regions and peripheral blood^{31–33}. In this preliminary imaging study, we aimed to determine if the same exposure to single and repeated mild blast overpressure that resulted in the abovementioned changes also induced structural changes that are detectable by DTI.

Results

We selected two of our previously tested post-injury termination time points, 2 h and 42 days, for the DTI analyses to mimic early and delayed clinical interventions. A manual region of interest (ROI) analysis was first used to assess hippocampal volume and fractional anisotropy (FA) in the hippocampus as shown in Fig. 1a. No significant differences were identified in hippocampal volume or FA values at either time point (Fig. 2). An anatomically defined ROI analysis

was then performed as shown in Fig. 1b–d. In rats terminated ~2 h after blast (or sham) exposure(s), no brain regions had a significant interaction for FA. However, axial diffusivity (AD) and radial diffusivity (RD) had significant interactions in regions of the stria terminalis, thalamic subregions, and the cerebellum. Post hoc analysis revealed that the single-injured (SI) and multiple-injured (MI) groups were significantly different from one another largely in the thalamus and thalamic nuclei. Regions exhibiting significant blast event-related differences (i.e., single vs. repeated blast) are shown in Fig. 3 and Table 1; mean DTI values for these regions are provided in Fig. 4. No brain regions exhibited significant ROI changes in rats terminated 42 days after blast (or sham) exposure(s).

Discussion

Elucidating the role of repeated mbTBI in the development of neurodegenerative conditions is a pressing issue for the military health care system. To that end, a better understanding of mbTBI pathobiology, the period of cerebral vulnerability between insults, and the synergistic effect of repeated injury is critical. In conducting a series of studies comparing single and repeated mild blast injury (5 overpressure exposures administered on consecutive days), we aimed to assess the extent of the damage accumulation in mbTBI (i.e., the

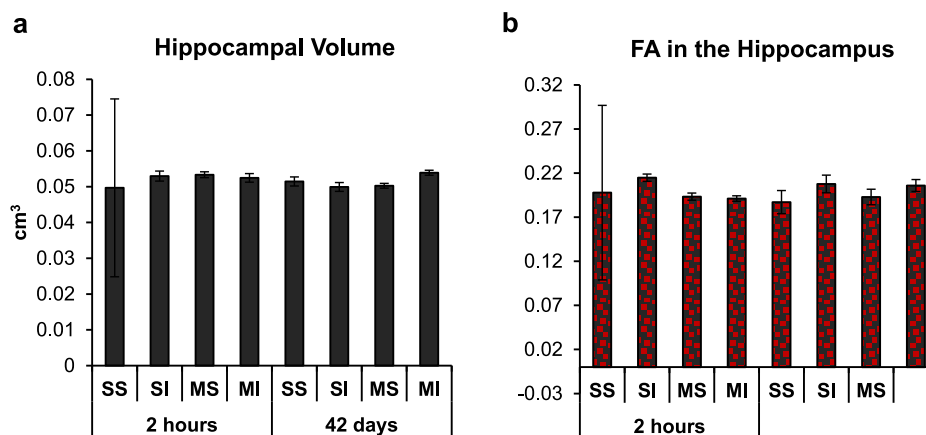


Figure 2 | Volumetric and DTI measures in the hippocampus. (a) Hippocampal volume (cm³) of sham (SS, single sham; MS, multiple sham) and injured (SI, single-injured; MI, multiple-injured) rats terminated at 2 h and 45 days after blast (or sham) exposure(s). (b) Fractional anisotropy (FA) in the hippocampi of rats at the same time points. Data are presented as the mean ± SEM.

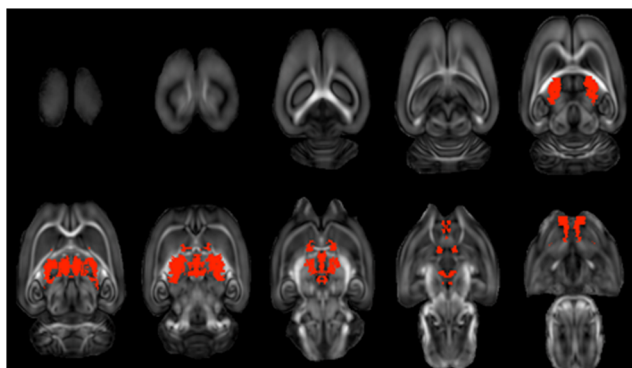


Figure 3 | Brain regions exhibiting significant ROI changes. Regions with a significant Blast x No. of Events interaction were first identified; those with significant differences between single-injured and multiple-injured rats (corrected for multiple comparisons) are shown in red.

cumulative effect of the injury) at different post-injury time points. Of particular interest to us is correlating cellular and molecular level changes with structural and neurocognitive changes toward a definitive diagnosis for mbTBI. The objective of this study was to determine if the exposure to single and repeated mild blast overpressure, which resulted in significant functional, cellular, and molecular changes, also induced structural changes that are detectable by *ex vivo* DTI.

Based on a number of bTBI studies that implicate the hippocampus in the development of neurobehavioral symptoms, we expected to detect injury-induced structural and/or volumetric changes in this region due to its involvement in TBI^{34,35}. We previously found significantly increased numbers of apoptotic, TUNEL-positive cells in the hilus and granular cell layer of the hippocampus as early as 2 h post-injury in both single- and multiple-injured rats³⁶. However, we found no significant changes in hippocampal volume or FA in the hippocampus in our current study. This discrepancy may be related to the current spatial resolution of DTI. Another plausible explanation is that even though we found significantly increased rates of cell death in the hippocampus, we also found a substantive gliotic response^{30,31,33,37}. Such astroglial hypertrophy can potentially compensate for the loss in volume caused by cell death.

A recent *ex vivo* DTI rodent study has shown that the microstructure of the hippocampus can be significantly affected in mbTBI²³. Consistent with impaired cognitive performance, FA values were significantly decreased in select brain regions of blast-exposed rats relative to their sham controls at 4 and 30 days post-injury. The affected brain regions included the hippocampus, thalamus, and brainstem. It is important to note, however, that the blast model and experimental design of our and the Budde et al. study are very different. Nonetheless, hippocampal abnormalities have been found in a number of clinical mbTBI studies using various imaging modalities^{12,15,17,38–40}.

Since no significant hippocampal changes were detected in our work, an automated, anatomical ROI analysis without a priori assumptions of affected regions was used to examine the brains²³. Compared to a voxel by voxel approach that includes thousands of independent statistical tests, the whole brain anatomical ROI approach reduces the number of statistical comparisons but avoids tedious manual definition of brain regions⁴¹. The results of this analysis demonstrated significant changes that are largely confined to midline thalamic structures and the cerebellum. Post hoc analysis revealed that SI and MI rats were significantly different from one another in the thalamus and thalamic nuclei. Previous bTBI studies also found changes in the thalamus using DTI²³ and histological methods⁴². Thalamus-mediated functions account for a significant number of the most frequently reported neurobehavioral symptoms in clinical mbTBI. Among the leading complaints are sleep and emotional disturbances as well as altered sensory sensitivities, both auditory and visual¹⁴.

Cerebellar abnormalities have been found in most human bTBI imaging studies^{12,15,16,43} and in a recent rodent bTBI study²⁴. These findings illustrate the region-specific vulnerability of the brain to different types of physical insults—an important albeit poorly understood issue in TBI. The cerebellum's susceptibility to injury maybe due to its anatomy; it is located in a relatively small sub-compartment of the skull and the ratio between cerebellar white and grey matters is different from that in the cerebrum. Primary blast injury mainly exerts damage at the interface of biological materials with differing physiochemical properties (e.g., grey and white matter). Indeed, white matter damage—including cerebellar white matter—has been found in virtually all human bTBI imaging studies. Functionally, the cerebellum is involved in certain cognitive and learning functions,

Table 1 | Brain regions exhibiting significant blast event-related effects at 2 h post-injury

Brain Region	Fractional Anisotropy		Axial Diffusivity				Radial Diffusivity			
	Blast x No. of Events Interaction		Blast x No. of Events Interaction		SI vs. MI <i>t</i> -Test		Blast x No. of Events Interaction		SI vs. MI <i>t</i> -Test	
	<i>F</i> value	<i>p</i> value ^a	<i>F</i> value	<i>p</i> value ^b	<i>t</i> value	<i>p</i> value ^b	<i>F</i> value	<i>p</i> value ^b	<i>t</i> value	<i>p</i> value ^b
<i>Stria Terminalis</i>	4.55	0.065	19.28	0.017	6.34	0.023	11.91	0.068	4.80	0.099
<i>Posterior Hypothalamic Nucleus</i>	1.25	0.296	13.56	0.043	3.78	0.145	13.57	0.048	4.06	0.189
<i>Islands of Calleja</i>	1.95	0.200	26.50	0.006	-9.89	0.004	34.55	0.003	-6.23	0.042
<i>Olfactory Tubercle</i>	1.02	0.341	35.79	0.002	-5.28	0.048	70.63	0.000	-7.95	0.010
<i>Ventral Nucleus of Thalamus</i>	0.98	0.352	29.78	0.004	9.02	0.007	20.89	0.014	6.81	0.026
<i>Lateral Dorsal Nucleus of Thalamus</i>	3.60	0.094	15.33	0.032	7.01	0.017	18.44	0.021	7.28	0.021
<i>Lateral Posterior Nucleus of Thalamus</i>	2.06	0.189	15.96	0.026	5.55	0.040	18.47	0.018	5.65	0.059
<i>Central Lateral Nucleus of Thalamus</i>	3.09	0.117	20.11	0.014	7.18	0.014	24.46	0.009	8.05	0.005
<i>Medial Dorsal Thalamus</i>	1.93	0.203	15.71	0.029	7.74	0.011	17.07	0.026	7.31	0.016
<i>Midline Thalamic Nuclei</i>	7.55	0.025	21.27	0.011	10.00	0.002	15.91	0.031	6.72	0.031
<i>Thalamus</i>	0.35	0.568	13.29	0.047	4.85	0.065	13.89	0.044	4.77	0.108
<i>Cerebellum</i>	4.24	0.073	17.26	0.022	-3.41	0.212	21.95	0.011	-5.05	0.089

^auncorrected.

^bfalse discovery rate corrected.

SI, single-injured (*n* = 3); MI, multiple-injured (*n* = 3).

Statistically significant differences between SI and MI rats are indicated in boldface.



hence the detected changes are consistent with clinically observed abnormalities^{44,45}.

Among the other affected brain structures is the stria terminalis, which serves as a major relay site within the hypothalamic-pituitary-adrenal axis⁴⁶. Similar changes were also found in the olfactory tubercle, including the islands of Calleja. The olfactory tubercle has been shown to play a role in behavioral response as it is interconnected with several brain regions with sensory and arousal/reward functions⁴⁷. In fact, injury to the islands as a result of restricted blood flow has been linked to a number of behavioral and emotional responses such as amnesia and changes in personality—behavioral changes that are not possible to assess in animal models.

A critical limitation toward better understanding human mbTBI is inherent variability as well as the unknown biophysical forces that are experienced during injury. Additionally, most existing DTI studies of veterans have been performed years after the injury. Animal models of mbTBI allow for direct testing of the many effects of blast wave characteristics under carefully controlled conditions⁴⁸. However, we currently have no clear understanding of how human years (physiologically and pathologically speaking) translate into rat months (or weeks). Furthermore, the lack of a consensus regarding a high fidelity experimental bTBI model—as demonstrated by the imaging findings obtained using various blast models—is a major impediment to studying the physical and biological effects of primary blast injury.

Another pressing issue is how DTI findings in mbTBI (or any other neurological disorder) relate to changes detectable by

proteomics or histology. We emphasize this point because although rats terminated at 42 days did not exhibit significant ROI changes as measured by DTI, proteomic analyses of plasma at the same time point showed significant and persistent molecular pathologies in SI as well as MI rats^{36,49}. These include inflammation, metabolic and vascular changes, neuronal and glial cell damage and/or death, and axonal damage.

A technical limitation of our study is the use of fixed tissues in *ex vivo* DTI, mainly due to altered diffusivity of water molecules. Nonetheless, previous studies have demonstrated that *ex vivo* DTI provides valuable structural information that correlates with *in vivo* changes albeit to a varying extent. This may partially account for the poor correlation between cellular changes obtained by conventional histology and volumetric/DTI measures in the hippocampus. It should be noted that animal *in vivo* imaging has its own issues with scanning times (and corresponding anesthesia times), image acquisition protocols, and motion artifacts being the major ones.

Despite the increased attention in recent years on blast as a mechanism of mTBI, the subject of how blast waves affect the brain along with diagnosing mbTBI are still a matter of considerable debate. The abovementioned caveats underline the importance of combining objective and clinically relevant outcome measures in experimental TBI to validate and correlate findings, to enable more direct comparisons of pathologies observed in animal and in clinical TBI research, and to enable the development of sensitive and specific diagnostics for mbTBI²⁹.

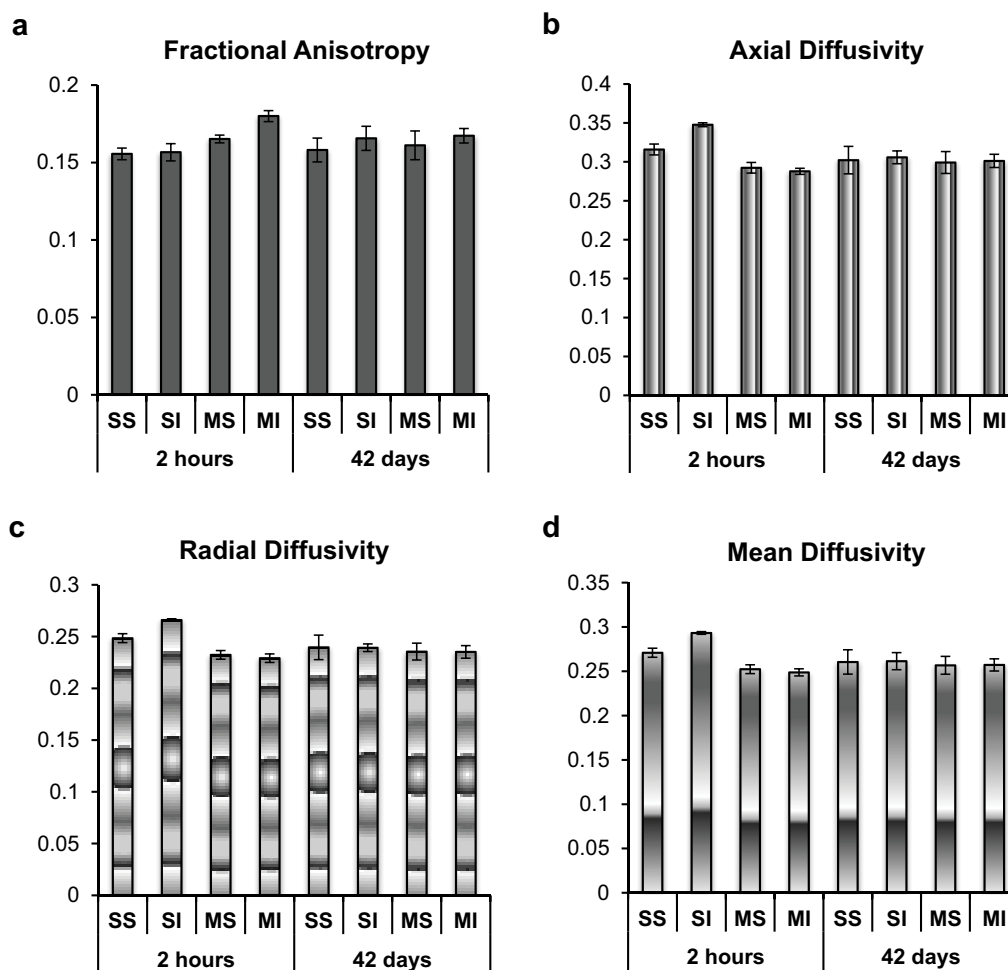


Figure 4 | Mean DTI values at the two time points. Data were extracted from each subject as a single value from the ROIs showing significance in the anatomical ROI analysis. Data are presented as the mean \pm SEM for each experimental group (SS, single sham; SI, single-injured; MS, multiple sham; MI, multiple-injured).



Methods

Animals and housing conditions. A total of 60 male Sprague Dawley rats (weight at arrival: 245–265 g) (Charles River Laboratories, Wilmington, MA) were used in the original experiments^{36,49}. All animals were housed in standard rat cages with a built-in filter in a reverse 12-h light 12-h dark cycle with food and water ad lib. Animals were handled according to protocol approved by the Institutional Animal Care and Use Committee at the Uniformed Services University (USU; Bethesda, MD).

Experimental groups and manipulations. All animals underwent a 5 day acclimation and handling period and were later assigned to the following groups: naïve, single sham (SS), single-injured (SI), multiple sham (MS), and multiple-injured (MI) as described earlier^{36,49}. Rat numbers in the early and late termination groups were: ($N = 30$; naïve = 3, SS = 6, SI = 7, MS = 6, MI = 8) and ($N = 30$; naïve = 3, SS = 6, SI = 7, MS = 6, MI = 8), respectively. Naïve rats were kept in the animal facility at USU without any manipulation for the duration of the studies. SS rats were transported once from USU to Walter Reed Army Institute of Research (Silver Spring, MD) and anesthetized in an induction chamber with a 4% isoflurane (Forane; Baxter Healthcare Corporation, Deerfield, IL) in air mixture delivered at 2 L/min for 6 min. MS rats were similarly transported and anesthetized once per day for 5 consecutive days. SI and MI rats underwent the same procedures as their respective sham controls in addition to receiving a single or multiple (5 total) mild blast exposure(s)^{36,49}.

Injury conditions. Anesthetized rats in chest protection (weight at injury: 300–330 g) were placed in the shock tube holder in a transverse prone position with the right side facing the direction of the membrane and the incidence of the blast waves. Blast overpressure was generated using a compressed air-driven shock tube yielding a single blast overpressure wave (average peak total pressure: ~137 kPa at the animal level) to produce a mild injury as described in detail^{31,37,50}. Following blast (or equivalent time spent anesthetized as a sham), animals were moved to an adjacent bench top for observation and then transported back to the USU animal facility at the conclusion of each injury day.

Preparation of specimens for imaging. A subset of animals from each experiment [(2 h termination: $n = 11$; SS = 2, SI = 3, MS = 3, MI = 3) and (42 day termination: $n = 16$; SS = 4, SI = 4, MS = 4, MI = 4)] was used for MRI/DTI analyses; all other animals were used for proteomics as described earlier^{36,49}. Rats were deeply anesthetized with isoflurane inhalant until a tail pinch produced no reflex movement, then transcardially perfused with cold phosphate-buffered saline (PBS) followed by a 4% paraformaldehyde in 1x PBS solution. The brains were removed and post-fixed in the same solution overnight at 4°C and then transferred to a 1x PBS solution containing 0.1% sodium azide until scanning. No hemorrhage or any other signs of macroscopic damage were detected in any of the animals.

Image acquisition. Fixed brains underwent ex vivo DTI within 2 days of perfusion fixation on a Bruker 7 T vertical bore system. Brains were immersed in susceptibility-matching fluid (Fomblin; Solvay Solexis, Inc., West Deptford, NJ) and inserted into a radiofrequency coil 3 cm in diameter. A three-echo diffusion-weighted spin echo sequence was employed (TR = 4 s; TE = 20 ms (first echo); 7.5 ms echo spacing) to acquire diffusion-weighted images ($b = 1200 \text{ s/mm}^2$) along 30 directions⁵¹ with diffusion gradient duration (δ) and separation (Δ) of 4 and 10 ms, respectively, along with 5 non diffusion-weighted images⁵². The slice thickness was 0.5 mm with an in-plane resolution of 0.234 mm² and a 30 mm² field of view (128² matrix). The full experiment required 6 h of continuous imaging. DTI data was reconstructed using a linear least squares fit to derive parameter maps of FA, AD, and RD using custom Matlab routines⁵³.

Data analysis. The analysis of MRI data included volumetric and DTI measures in the hippocampus and an anatomical ROI analysis of DTI data without a priori assumptions of affected regions. Hippocampal volume and FA in the hippocampus were derived from manual segmentation of the hippocampus on T2-weighted and FA maps, respectively, by an operator blinded to animal conditions. For unbiased quantification of DTI measures using anatomically based ROIs, DTI volumes from all subjects were first registered to a common space using an iterative, tensor-based registration routine implemented in DTI-TK⁵⁴. Rigid-body, affine, and diffeomorphic (piecewise affine) methods were used in succession to progressively improve registration accuracy, as this approach has been shown to be superior to other routines⁵⁵. The final image resolution was $120 \times 120 \times 500 \mu\text{m}^3$. Anatomical ROIs were derived from a digital rat brain atlas included as part of the Medical Image Visualization and Analysis Software (MIVA) software package⁵⁶. The regions consisted of 87 subregions of the brain initially derived from the Paxinos Rat brain atlas⁵⁷. A mask of white matter regions derived from the atlas was registered to a mask of white matter regions derived from DTI by thresholding the FA maps at 0.2. An FA value of 0.2 was chosen empirically since it effectively masked the white matter tracts. It should be noted that this threshold value was used for the registration of the ROIs, not for quantification. Registration employed a point-set based registration metric incorporated into Advanced Normalization Tools (ANTS) software package, including elastic warping⁵⁸. The resulting overlap demonstrated high correspondence between the DTI and atlas-based white matter structures (Fig. 1C). The mean FA, AD, and RD within each ROI were derived from each of the registered DTI volumes from each subject for subsequent statistical analysis (Fig. 4).

Statistical analysis. Twenty-seven animals were used for the analyses (2 h termination, $N = 11$; 42 day termination, $N = 16$). A mixed-effect ANOVA was first performed to identify any significant effects of left/right (L/R) asymmetry. Since none of the brain regions exhibited a significant Blast x No. of Events x Side (L/R) interaction, the effect of side was collapsed for all subsequent analyses. For hippocampal volume and FA in the hippocampus, ANOVAs followed by Tukey's HSD test were performed separately at each time point. Subsequently, a one-way ANOVA was performed for each condition across the two time points.

For DTI, a two-way ANOVA was performed to compare the main effects of Blast x No. of Events interaction. Regions that exhibited a significant interaction were subjected to post-hoc analysis using a Student's *t*-test to compare the SI and MI groups. All statistical tests were corrected for multiple comparisons (87 individual ROIs) by controlling for the false discovery rate⁵⁹. A Spearman correlation analysis was used to identify brain regions significantly correlated to either the number of blast events or the number of sham events. A corrected *p* value of 0.05 was considered significant for all tests.

- Laker, S. R. Epidemiology of concussion and mild traumatic brain injury. *PM R* **3**, S354–358; DOI:10.1016/j.pmrj.2011.07.017 (2011).
- Hendricks, A. M. *et al.* Screening for mild traumatic brain injury in OEF/OIF deployed US military: an empirical assessment of VHA's experience. *Brain. Inj.* **27**, 125–134; DOI:10.3109/02699052.2012.729284 (2013).
- Vanderploeg, R. D. *et al.* Health outcomes associated with military deployment: mild traumatic brain injury, blast, trauma, and combat associations in the Florida National Guard. *Arch. Phys. Med. Rehabil.* **93**, 1887–1895; DOI:10.1016/j.apmr.2012.05.024 (2012).
- Xydakis, M. S., Ling, G. S., Mulligan, L. P., Olsen, C. H. & Dorlac, W. C. Epidemiologic aspects of traumatic brain injury in acute combat casualties at a major military medical center: a cohort study. *Ann. Neurol.* **72**, 673–681; DOI:10.1002/ana.23757 (2012).
- Brenner, L. A., Vanderploeg, R. D. & Terrio, H. Assessment and diagnosis of mild traumatic brain injury, posttraumatic stress disorder, and other polytrauma conditions: burden of adversity hypothesis. *Rehabil. Psychol.* **54**, 239–246; DOI:10.1037/a0016908 (2009).
- Stern, R. A. *et al.* Long-term consequences of repetitive brain trauma: chronic traumatic encephalopathy. *PM R* **3**, S460–467; DOI:10.1016/j.pmrj.2011.08.008 (2011).
- Aoki, Y., Inokuchi, R., Gunshin, M., Yahagi, N. & Suwa, H. Diffusion tensor imaging studies of mild traumatic brain injury: a meta-analysis. *J. Neurol. Neurosurg. Psychiatry* **83**, 870–876; DOI:10.1136/jnnp-2012-302742 (2012).
- Shenton, M. E. *et al.* A review of magnetic resonance imaging and diffusion tensor imaging findings in mild traumatic brain injury. *Brain Imaging Behav.* **6**, 137–192; DOI:10.1007/s11682-012-9156-5 (2012).
- Voelbel, G. T., Genova, H. M., Chiaravallotti, N. D. & Hoptman, M. J. Diffusion tensor imaging of traumatic brain injury review: implications for neurorehabilitation. *NeuroRehabilitation* **31**, 281–293; DOI:10.3233/nre-2012-0796 (2012).
- Xiong, K. L., Zhu, Y. S. & Zhang, W. G. Diffusion tensor imaging and magnetic resonance spectroscopy in traumatic brain injury: a review of recent literature. *Brain Imaging Behav.* DOI:10.1007/s11682-013-9288-2 (2014).
- Benzinger, T. L. *et al.* Blast-related brain injury: imaging for clinical and research applications: report of the 2008 st. Louis workshop. *J. Neurotrauma* **26**, 2127–2144; DOI:10.1089/neu.2009-0885 (2009).
- Levin, H. S. *et al.* Diffusion tensor imaging of mild to moderate blast-related traumatic brain injury and its sequelae. *J. Neurotrauma* **27**, 683–694; DOI:10.1089/neu.2009.1073 (2010).
- Mendez, M. F. *et al.* Mild traumatic brain injury from primary blast vs. blunt forces: post-concussion consequences and functional neuroimaging. *NeuroRehabilitation* **32**, 397–407; DOI:10.3233/nre-130861 (2013).
- Petrie, E. C. *et al.* Neuroimaging, behavioral, and psychological sequelae of repetitive combined blast/impact mild traumatic brain injury in Iraq and Afghanistan war veterans. *J. Neurotrauma* **31**, 425–436; DOI:10.1089/neu.2013.2952 (2014).
- Matthews, S. C. *et al.* A multimodal imaging study in U.S. veterans of Operations Iraqi and Enduring Freedom with and without major depression after blast-related concussion. *Neuroimage* **54**, S69–75; DOI:10.1016/j.neuroimage.2010.04.269 (2011).
- Mac Donald, C. *et al.* Cerebellar white matter abnormalities following primary blast injury in US military personnel. *PLoS ONE* **8**, e55823; DOI:10.1371/journal.pone.0055823 (2013).
- Matthews, S. C., Spadoni, A. D., Lohr, J. B., Strigo, I. A. & Simmons, A. N. Diffusion tensor imaging evidence of white matter disruption associated with loss versus alteration of consciousness in warfighters exposed to combat in Operations Enduring and Iraqi Freedom. *Psychiatry Res.* **204**, 149–154; DOI:10.1016/j.psychres.2012.04.018 (2012).
- Bennett, R. E., Mac Donald, C. L. & Brody, D. L. Diffusion tensor imaging detects axonal injury in a mouse model of repetitive closed-skull traumatic brain injury. *Neurosci. Lett.* **513**, 160–165; DOI:10.1016/j.neulet.2012.02.024 (2012).
- Albensi, B. C. *et al.* Diffusion and high resolution MRI of traumatic brain injury in rats: time course and correlation with histology. *Exp. Neurol.* **162**, 61–72; DOI:10.1006/exnr.2000.7256 (2000).



20. Cernak, I. *et al.* The pathobiology of moderate diffuse traumatic brain injury as identified using a new experimental model of injury in rats. *Neurobiol. Dis.* **17**, 29–43; DOI:10.1016/j.nbd.2004.05.011 (2004).
21. Henninger, N. *et al.* Differential recovery of behavioral status and brain function assessed with functional magnetic resonance imaging after mild traumatic brain injury in the rat. *Crit. Care Med.* **35**, 2607–2614; DOI:10.1097/01.ccm.0000286395.79654.8d (2007).
22. van de Looij, Y. *et al.* Diffusion tensor imaging of diffuse axonal injury in a rat brain trauma model. *NMR Biomed.* **25**, 93–103; DOI:10.1002/nbm.1721 (2012).
23. Budde, M. D. *et al.* Primary blast traumatic brain injury in the rat: relating diffusion tensor imaging and behavior. *Front. Neurol.* **4**, 154; DOI:10.3389/fneur.2013.00154 (2013).
24. Calabrese, E. *et al.* Diffusion tensor imaging reveals white matter injury in a rat model of repetitive blast-induced traumatic brain injury. *J. Neurotrauma.* DOI:10.1089/neu.2013.3144 (2014).
25. Morey, R. A. *et al.* Effects of chronic mild traumatic brain injury on white matter integrity in Iraq and Afghanistan war veterans. *Hum. Brain Mapp.* **34**, 2986–2999; DOI:10.1002/hbm.22117 (2013).
26. Di Battista, A. P., Rhind, S. G. & Baker, A. J. Application of blood-based biomarkers in human mild traumatic brain injury. *Front. Neurol.* **4**, 44; DOI:10.3389/fneur.2013.00044 (2013).
27. Kobeissy, F. H. *et al.* Neuroproteomics and systems biology-based discovery of protein biomarkers for traumatic brain injury and clinical validation. *Proteomics Clin. Appl.* **2**, 1467–1483; DOI:10.1002/prca.200800011 (2008).
28. Wang, K. K. *et al.* Proteomic identification of biomarkers of traumatic brain injury. *Expert Rev. Proteomics* **2**, 603–614; DOI:10.1586/14789450.2.4.603 (2005).
29. Agoston, D. V., Risling, M. & Bellander, B. M. Bench-to-bedside and bedside back to the bench; coordinating clinical and experimental traumatic brain injury studies. *Front. Neurol.* **3**, 3; DOI:10.3389/fneur.2012.00003 (2012).
30. Kwon, S. K. *et al.* Stress and traumatic brain injury: a behavioral, proteomics, and histological study. *Front. Neurol.* **2**, 12; DOI:10.3389/fneur.2011.00012 (2011).
31. Kamnaksh, A. *et al.* Factors affecting blast traumatic brain injury. *J. Neurotrauma* **28**, 2145–2153; DOI:10.1089/neu.2011.1983 (2011).
32. Kovesdi, E. *et al.* The effect of enriched environment on the outcome of traumatic brain injury: a behavioral, proteomics, and histological study. *Front. Neurosci.* **5**, 42; DOI:10.3389/fnins.2011.00042 (2011).
33. Kovesdi, E. *et al.* Acute minocycline treatment mitigates the symptoms of mild blast-induced traumatic brain injury. *Front. Neurol.* **3**, 111; DOI:10.3389/fneur.2012.00111 (2012).
34. Orrison, W. W. *et al.* Traumatic brain injury: a review and high-field MRI findings in 100 unarmed combatants using a literature-based checklist approach. *J. Neurotrauma* **26**, 689–701; DOI:10.1089/neu.2008.0636 (2009).
35. Bigler, E. D. Quantitative magnetic resonance imaging in traumatic brain injury. *J. Head Trauma Rehabil.* **16**, 117–134 (2001).
36. Kamnaksh, A. *et al.* Neurobehavioral, cellular, and molecular consequences of single and multiple mild blast exposure. *Electrophoresis* **33**, 3680–3692; DOI:10.1002/elps.201200319 (2012).
37. Ahmed, F. *et al.* Time-dependent changes of protein biomarker levels in the cerebrospinal fluid after blast traumatic brain injury. *Electrophoresis* **33**, 3705–3711; DOI:10.1002/elps.201200299 (2012).
38. Hetherington, H. P. *et al.* MRSI of the medial temporal lobe at 7 T in explosive blast mild traumatic brain injury. *Magn. Reson. Med.* **71**, 1358–1367; DOI:10.1002/mrm.24814 (2014).
39. Masel, B. E. *et al.* Galveston Brain Injury Conference 2010: clinical and experimental aspects of blast injury. *J. Neurotrauma* **29**, 2143–2171; DOI:10.1089/neu.2011.2258 (2012).
40. Scheibel, R. S. *et al.* Altered brain activation in military personnel with one or more traumatic brain injuries following blast. *J. Int. Neuropsychol. Soc.* **18**, 89–100; DOI:10.1017/s1355617711001433 (2012).
41. Lu, H. *et al.* Registering and analyzing rat fMRI data in the stereotaxic framework by exploiting intrinsic anatomical features. *Magn. Reson. Imaging* **28**, 146–152; DOI:10.1016/j.mri.2009.05.019 (2010).
42. Goldstein, L. E. *et al.* Chronic traumatic encephalopathy in blast-exposed military veterans and a blast neurotrauma mouse model. *Sci. Transl. Med.* **4**, 134ra60; DOI:10.1126/scitranslmed.3003716 (2012).
43. Jorge, R. E. *et al.* White matter abnormalities in veterans with mild traumatic brain injury. *Am. J. Psychiatry* **169**, 1284–1291; DOI:10.1176/appi.ajp.2012.12050600 (2012).
44. Stoodley, C. J. The cerebellum and cognition: evidence from functional imaging studies. *Cerebellum* **11**, 352–365; DOI:10.1007/s12311-011-0260-7 (2012).
45. Van Overwalle, F., Baetens, K., Marien, P. & Vandekerckhove, M. Social cognition and the cerebellum: A meta-analysis of over 350 fMRI studies. *Neuroimage* **86**, 554–572; DOI:10.1016/j.neuroimage.2013.09.033 (2014).
46. Crestani, C. C. *et al.* Mechanisms in the bed nucleus of the stria terminalis involved in control of autonomic and neuroendocrine functions: a review. *Curr. Neuropharmacol.* **11**, 141–159; DOI:10.2174/1570159x11311020002 (2013).
47. Rodrigo, J. *et al.* Physiology and pathophysiology of nitric oxide in the nervous system, with special mention of the islands of Calleja and the circumventricular organs. *Histol. Histopathol.* **17**, 973–1003 (2002).
48. Bass, C. R. *et al.* Brain injuries from blast. *Ann. Biomed. Eng.* **40**, 185–202; DOI:10.1007/s10439-011-0424-0 (2012).
49. Ahmed, F. A., Kamnaksh, A., Kovesdi, E., Long, J. B. & Agoston, D. V. Long-term consequences of single and multiple mild blast exposure on select physiological parameters and blood-based biomarkers. *Electrophoresis* **34**, 2229–2233; DOI:10.1002/elps.201300077 (2013).
50. Long, J. B. *et al.* Blast overpressure in rats: recreating a battlefield injury in the laboratory. *J. Neurotrauma* **26**, 827–840; DOI:10.1089/neu.2008.0748 (2009).
51. Hasan, K. M., Parker, D. L. & Alexander, A. L. Comparison of gradient encoding schemes for diffusion-tensor MRI. *J. Magn. Reson. Imaging* **13**, 769–780 (2001).
52. Budde, M. D. & Frank, J. A. Examining brain microstructure using structure tensor analysis of histological sections. *Neuroimage* **63**, 1–10; DOI:10.1016/j.neuroimage.2012.06.042 (2012).
53. Budde, M. D., Janes, L., Gold, E., Turtzo, L. C. & Frank, J. A. The contribution of gliosis to diffusion tensor anisotropy and tractography following traumatic brain injury: validation in the rat using Fourier analysis of stained tissue sections. *Brain* **134**, 2248–2260; DOI:10.1093/brain/awr161 (2011).
54. Zhang, H., Yushkevich, P. A., Alexander, D. C. & Gee, J. C. Deformable registration of diffusion tensor MR images with explicit orientation optimization. *Med. Image Anal.* **10**, 764–785; DOI:10.1016/j.media.2006.06.004 (2006).
55. Adluru, N. *et al.* A diffusion tensor brain template for rhesus macaques. *Neuroimage* **59**, 306–318; DOI:10.1016/j.neuroimage.2011.07.029 (2012).
56. Ferris, C. F. *et al.* Functional magnetic resonance imaging in awake animals. *Rev. Neurosci.* **22**, 665–674; DOI:10.1515/rns.2011.050 (2011).
57. Paxinos, G. & Watson, C. *The Rat Brain in Stereotaxic Coordinates*. (Academic Press, 2007).
58. Avants, B. B. *et al.* A reproducible evaluation of ANTs similarity metric performance in brain image registration. *Neuroimage*, **54**, 2033–2044; DOI:10.1016/j.neuroimage.2010.09.025 (2011).
59. Benjamini, Y., Drai, D., Elmer, G., Kafkafi, N. & Golani, I. Controlling the false discovery rate in behavior genetics research. *Behav. Brain Res.* **125**, 279–284 (2001).

Acknowledgments

We thank the Neurotrauma Team at the Walter Reed Army Institute of Research for their technical help during the exposures, along with Eric Gold and Lindsay Janes for assistance with the MRI experiments. This work was supported by the Center for Neuroscience and Regenerative Medicine grant number G1703F.

Author contributions

A.K. and E.K. carried out animal studies, including the preparation of specimens for imaging. J.L. designed and supervised blast overpressure exposures at Walter Reed. M.B. performed and analyzed MRI/DTI measures under J.F.'s supervision at the NIH. A.K., M.B., and D.A. wrote the main manuscript text; A.K. and M.B. generated and formatted figures 1–4 and table 1. A.K. and D.A. reviewed the manuscript prior to submission.

Additional information

Competing financial interests: The authors declare no competing financial interests.

How to cite this article: Kamnaksh, A. *et al.* Diffusion Tensor Imaging Reveals Acute Subcortical Changes after Mild Blast-Induced Traumatic Brain Injury. *Sci. Rep.* **4**, 4809; DOI:10.1038/srep04809 (2014).



This work is licensed under a Creative Commons Attribution-NonCommercial-NoDerivs 3.0 Unported License. The images in this article are included in the article's Creative Commons license, unless indicated otherwise in the image credit; if the image is not included under the Creative Commons license, users will need to obtain permission from the license holder in order to reproduce the image. To view a copy of this license, visit <http://creativecommons.org/licenses/by-nc-nd/3.0/>